

Pseudo slug flow in viscous oil systems – experiments and modelling with LedaFlow

Jørn Kjølås, Ivar E. Smith and Christian Brekken
SINTEF, Norway

ABSTRACT

An experimental two-phase flow campaign with a viscous oil (100 cP) was conducted in the Large Scale 8" loop at the SINTEF Multiphase Flow Laboratory. The loop consisted of three main test sections, with pipe inclinations 0, 0.5 and 90 degrees, and with approximate lengths of 380 m, 380 m and 50 m, respectively. The experiments were performed at system pressures 20, 45 and 85 bara. The primary focus of the campaign was on liquid dominated flows in horizontal/near-horizontal pipes, with particular emphasis on the laminar-to-turbulent transition in the liquid. The main instruments were DP-cells for pressure drop measurements, and narrow beam gamma densitometers to measure the liquid height. In addition, traversing gamma densitometers were mounted on each of the two near-horizontal sections to measure the time-averaged liquid distribution and volume fractions.

In this campaign, it was found that at high pressure, the slug flow region was very narrow. In particular, at low gas-liquid ratios, the prevailing flow regime was determined to be a kind of "pseudo slug flow", which was characterized by large waves that did not quite extend to the top of the line. Simulations with the commercial multiphase simulator LedaFlow [1] did not reproduce this at the time, and the penalty for this discrepancy was that the predicted pressure drop was too high. Consequently, it was concluded that the physical models in LedaFlow needed improvement to predict these conditions better. Through detailed analysis of the experimental data, it was found that at these conditions, slugs were often not able to form because the waves did not have sufficient inertia to sustain a slug front. This limitation was not accounted for in the flow regime criteria in LedaFlow, so to improve the situation, the existing slug flow model in LedaFlow was generalized to cover pseudo slug flow in addition to regular slug flow. By introducing this new pseudo slug flow regime, the pressure drop predictions in viscous oil systems became significantly more accurate than before.

Nomenclature

D	Inner pipe diameter [m]
Fr	Froude number = $u/\sqrt{g'D}$
Fr_{film}	Liquid film Froude number on the super-critical side of a slug/wave front
$Fr_{supercrit}$	Liquid film Froude number on the super-critical side of a hydraulic jump
g	Acceleration of gravity [m/s ²]
g'	Density-corrected acceleration of gravity = $\Delta\rho g/\rho_l$ [m/s ²]
h_{film}	Liquid film height [m]
$h_{subcrit}$	Liquid height on the sub-critical side of a hydraulic jump [m]

$h_{supercrit}$	Liquid height on the super-critical side of a hydraulic jump [m]
h_{wave}	Wave height [m]
$u_{cg,wave}$	Velocity of the gas over a wave [m/s]
$u_{dg,wave}$	Velocity of the dispersed gas bubbles in a wave [m/s]
u_F	Wave front velocity [m/s]
$u_{supercrit}$	Liquid velocity on the super-critical side of a hydraulic jump [m/s]
u_{wave}	Wave velocity [m/s]
USG	Superficial gas velocity [m/s]
USG^*	Normalized superficial gas velocity [-]
USL	Superficial liquid velocity [m/s]
$\alpha_{cg,wave}$	Continuous gas volume fraction over a wave
$\alpha_{dg,wave}$	Dispersed gas volume fraction in a wave
α_{film}	Liquid film volume fraction on the supercritical side of a hydraulic jump
α_g	Gas volume fraction
α_g^s	Slug gas volume fraction
α_{cl}	Liquid zone volume fraction
ρ_g	Gas density [kg/m ³]
ρ_l	Liquid density [kg/m ³]

1 INTRODUCTION

Heavy oils make up around 70% of the world's total oil resources, and many large field developments target these reserves [2]. One of the main challenges with producing heavy oils is related to the associated high viscosities, which can yield large frictional pressure drops, leading to problems in transporting the oil over long distances. Often, transportation requires viscosity reduction techniques, such as dilution by adding light oil, or thermal assistance. The ability to predict the pressure drop in viscous oil systems is therefore of considerable importance, as the design of the associated transport processes often relies heavily on simulations using multiphase models. For instance, in the case of viscosity reduction through heating, one needs to consider the economic aspects of the required power consumption, which can reduce the prevailing profit margin. In such cases, it is crucial to obtain realistic predictions of the total flow resistance at various temperatures/viscosities, which in effect determines the amount of heating required, and the economic viability of the project.

Conventional oil resources are becoming more scarce, and because of the relative abundance of heavy oil deposits, there has been an increasing interest towards investing in heavy-oil reservoirs [2]. Therefore, many experimental studies targeting two-phase gas-liquid flows with viscous oils have been conducted in recent years to provide empirical data as design/decision support for such developments [3] [4] [5] [6] [7] [8]. A common feature of most of these studies is that the gas density was low (typically 1-2 kg/m³), and the pipe diameter was small ($D < 60$ mm). These experiments yield interesting results, especially in terms of shedding light on viscosity-sensitive phenomena. However, empirical closure laws based on such data are probably not very suitable for more realistic conditions, where the pressure is high and the diameter large. Indeed, it is well known that the flow regime map changes dramatically when moving from low-pressure to high-pressure conditions [9]. Also, extrapolating models based only small pipe diameter data is a major concern, because certain physical phenomena might only be readily observable at large diameters. In the current paper, we show that these scaling issues are indeed very important, as the central phenomenon discussed here occurs mainly for large pipe diameters at high pressure.

In terms of modelling, many closure laws have been proposed for the low Reynolds number range based on various viscous oil data sets. For instance, Jeyachandra et al. [10] proposed a new model for the drift velocity of large bubbles for high-viscosity liquids. Kora et al. [11] analysed slug flow experiments with viscous oils, and suggested a new correlation for predicting the slug void fraction. Gokcal et al. [12] also performed slug analyses on viscous oil experiments, and subsequently proposed a slug frequency correlation based on their findings. Also worth mentioning is the slug bubble velocity model developed by Nuland [6], covering all Reynolds numbers.

There has also been some work related to constructing unified models for viscous oil systems. Nossen & Lawrence [13] assembled various published closure laws from the literature into a unified point model, and compared the prevailing predictions with the experimental data produced by Gokcal [7]. The authors were able to match the measured pressure drops very well after introducing an ad hoc energy dissipation term associated with the liquid acceleration at slug fronts. Smith et al. [14] conducted a similar exercise using a small-diameter data set with high gas density, and they were also able to obtain good agreement after re-tuning some of the closure laws found in the literature.

Current commercial multiphase models have for the most part targeted conventional oils with low viscosities, and it is known that closure laws tailored towards such systems do not necessarily extrapolate well to viscous oil systems [15]. In particular, models developed using data at fully turbulent conditions may exhibit poor accuracy at low Reynolds numbers. Motivated by this challenge, a new experimental project was launched in 2012 [16], aiming at producing high-quality two-phase gas-oil data with a viscous oil at realistic conditions (high pressure and large diameter). This data will be described in the next section.

Following this experimental programme, a viscous oil modelling project was initiated [17]. The newly acquired viscous oil data was used to derive closure laws that would yield reliable predictions in high-viscosity systems. Several new closure models were derived as part of the post-experimental work. In this paper, we describe what we found to be one of the most critical aspects: the modelling of pseudo slug flow for high-viscosity multiphase flows.

2 EXPERIMENTAL SETUP AND RESULTS

The experiments described were carried out at the SINTEF Multiphase Flow Laboratory at Tiller, Norway, as part of the VOMS project [16]. The aim of these experiments was to produce industrially relevant two-phase flow data using a high-viscosity liquid. The primary novelty of these experiments was that they were conducted at high pressure (20, 45 and 85 bara), using a large diameter pipe (189 mm), yielding conditions that are close to those encountered in typical heavy oil transport applications. The fluid temperatures were carefully monitored and controlled along the entire flow loop, and the maximum accepted deviation from the nominal temperature of 20°C was 0.5°C. A photograph of the laboratory is shown in Figure 1.

The experimental setup consisted of three main test sections: One horizontal section (360 m), one 0.5° inclined section (374 m), followed by 48 m tall vertical riser. In this paper, we only address the results obtained in the near-horizontal pipes (0° and 0.5°).

The horizontal test section was preceded by a 30 m long section with pipe angle -5°. The purpose of this downward sloping pipe section was to facilitate stratified flow at the entrance of the horizontal pipe. In this way, any slugs in the horizontal pipe would have to be generated spontaneously, and not introduced in the gas-liquid mixing mechanism.

The experiments were conducted using Nitrogen as the gas phase, and Nexbase 3080 as the liquid phase. The associated fluid properties are listed in Table 1.



Figure 1: SINTEF's Multiphase Flow Laboratory at Tiller, Norway.

Table 1: Fluid properties at 20, 45 and 85 bara and 20°C

Nominal pressure [bara]	Liquid density [kg/m ³]	Gas density [kg/m ³]	Liquid viscosity [cP]	Gas viscosity [cP]
20	844.8	23.5	98.7	0.018
45	846.0	51.9	94.3	0.018
85	847.5	97.1	86.6	0.019

2.1 Measurements

For low gas flow rates (<1 m/s), the gas flow rate was measured using a Coriolis meter (Micro Motion CMF050 [18]), while for higher rates, an ultrasonic meter was used. The liquid rate was measured using two Coriolis meters (CMF400 and CMF200), selecting the most suitable one in each experiment, depending on the flow rate of interest.

The gas properties were calculated from the measured pressure and temperature using reference values obtained from NIST [19]. The liquid density was measured by the Coriolis meters, and the liquid viscosity was logged online using a viscosimeter. The viscosimeter measurements were corroborated by offline rheometer measurements as well as pressure drop measurements in single phase liquid flow. Temperature sensors were mounted at the bottom of the pipe at the start and end of each test section, so that the liquid temperature, and subsequently the viscosity, could be obtained and controlled.

The pressure drop was measured using DP-cells attached between the test section and a common reference line to obtain pressure gradients at various positions along the pipe.

There were six DP-cells mounted on the horizontal line, and five DP-cells on the inclined test section. The liquid height was measured with high temporal resolution using vertically oriented narrow-beam gamma densitometers. There were four liquid height measurements on each test section. In addition, traversing gamma densitometers were installed near the end of each test section to measure vertical profiles of the time-averaged liquid volume fraction. The most important measurement uncertainties are listed in Table 2.

Table 2: Measurement uncertainties (expressed as one standard deviation).

Quantity	Uncertainty	Quantity	Uncertainty
Liquid density	1.4 kg/m ³	<i>USG</i>	1.2 %
Gas density	0.1 kg/m ³	Liquid holdup	~0.02
<i>USL</i>	0.4 %	Pressure drop	3-5 Pa/m

2.2 Sample results

The experimental campaign covered a broad range of conditions and flow rates. In this paper, we focus on data points with relatively high liquid rates ($USL \geq 1$ m/s) and moderate gas rates ($USG < 5$ m/s). The reason for selecting these ranges was that pseudo slug flow was one of the prevailing flow regimes in this domain. These conditions are also quite relevant for typical heavy oil deposits, where the gas-liquid ratio tends to be relatively low [2].

Figure 2 shows some experimental results obtained in the inclined section at 45 bara pressure. We have here plotted the liquid holdup (volume fraction) and the pressure drop against USG^* for three different liquid rates ($USL=1, 1.5$ and 2 m/s). Here, USG^* is the superficial gas velocity, normalized by an undisclosed factor for confidentiality purposes.

The markers are the measured values, and the lines represent simulation results obtained with LedaFlow 2.3. From these graphs we see that the predictions with LedaFlow 2.3 are quite close to the measurements for $USG^* \geq 0.5$, but under this gas flow rate, the predicted pressure drop is too high. In the next section, we will clarify the reason for these discrepancies, and introduce new modelling concepts that in turn improves the simulator performance.

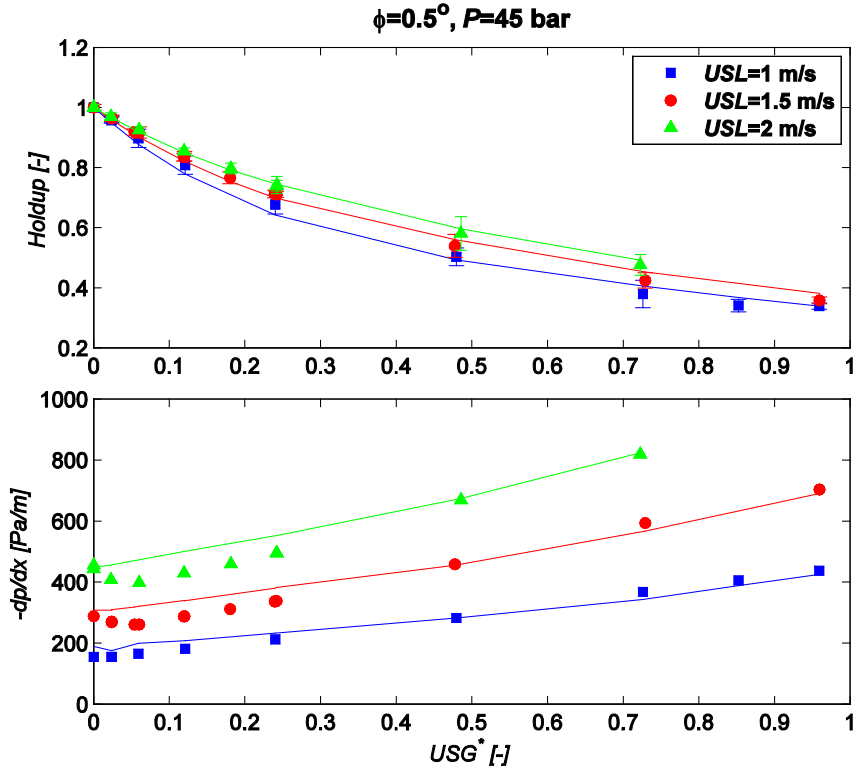


Figure 2: Liquid holdup and pressure drop plotted against USG^* in the 0.5° inclined section at 45 bar pressure. The lines are simulation results obtained using LedaFlow 2.3.

3 DATA ANALYSIS AND MODELLING

Upon examining the liquid height time series obtained from gamma densitometers for the cases with low USG , it was found that the flow regime here was a kind of stratified flow with very large waves. In this paper, we designate this flow regime as "pseudo slug flow", because the main characteristics of the flow in these cases resembles slug flow. Specifically, it was found that the average holdup in this flow regime matched the expected values for slug flow.

Figure 3 shows some of the data points from Figure 2, more specifically the series with $USL=1.5 \text{ m/s}$. In these graphs, we have used separate markers to indicate the experimental flow regime, and we see that the flow regime changes from slug flow to pseudo slug flow when decreasing USG^* from 0.48 to 0.24. This is supported by the liquid height signals shown in Figure 4, where we see a clear difference in the time trace signatures when comparing these two gas rates.

The blue line in Figure 3 shows the simulation results obtained using LedaFlow 2.3, and the predicted flow regime is slug flow for all the points. Looking at the bottom graph in Figure 3, we see that LedaFlow predicts the pressure drop well for the slug flow experiments, but overpredicts the pressure drop when the flow regime is not slug flow. Consequently, it appears that the errors in the pressure drop predictions are a consequence

of wrong flow regime predictions in the simulator. Indeed, waves are expected to exert less friction than slugs because they do not wet the whole pipe perimeter, so it makes sense that the pressure drop predictions are too high in these cases.

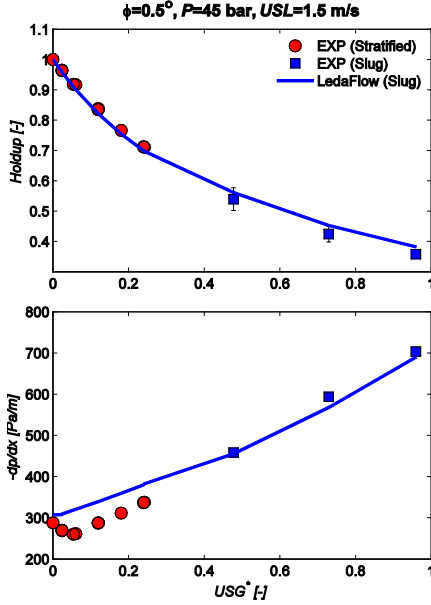


Figure 3: Holdup and pressure drop vs. USG^* .

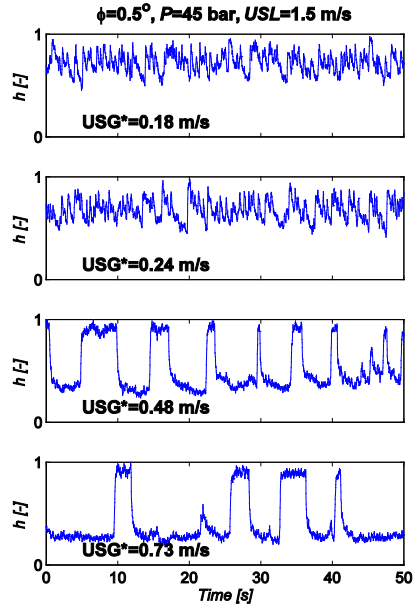


Figure 4: Liquid height vs. time.

In LedaFlow, the "minimum slip" criterion is used to determine if the flow regime is slug flow [20]. This criterion is equivalent to stating that "If there is enough liquid in the pipe for a slug to survive, then the prevailing flow regime is slug flow". However, in the cases presented in Figure 3, this criterion apparently fails, suggesting that the criterion, although a necessary one, is not sufficient.

Our proposed explanation for the discrepancies in the flow regime predictions, and subsequently the poor pressure drop predictions, is that the conditions are such that slug fronts cannot be maintained. Essentially, a slug front can be viewed as a hydraulic jump, where the flow is subcritical ($Fr < 1$) on one side of the jump (in the slug), and supercritical ($Fr > 1$) on the other side (in the liquid film in front of the slug). The height of a hydraulic jump depends on the ratio of inertial forces and the competing gravity forces. For channel flow, the liquid height $h_{subcrit}$ on the subcritical side is given by the following equation [21]:

$$h_{subcrit} = h_{supercrit} \cdot \frac{\sqrt{1 + 8Fr_{supercrit}^2} - 1}{2} \quad (1)$$

Here, $h_{supercrit}$ is the liquid height on the supercritical side of the jump, and $Fr_{supercrit}$ is the associated Froude number:

$$Fr_{supercrit}^2 = \frac{u_{supercrit}^2}{g'h_{supercrit}} \quad (2)$$

Here, $u_{supercrit}$ is the liquid velocity on the supercritical side, and g' is the density-corrected gravity acceleration.

Equation (2) applies to a stationary hydraulic jump. When applying this analysis to a slug/wave front, we want to choose a reference frame in which the slug/wave front is stationary, i.e. a reference frame travelling at the wave front velocity u_F . The Froude number for the slug/wave front then becomes:

$$Fr_{supercrit}^2 = \frac{(u_F - u_{supercrit})^2}{g'h_{supercrit}} \quad (3)$$

For the sake of clarity, we may again point out that for a slug/wave front, the slug/wave represents the subcritical side of the jump, and the film in front of the slug/wave represents the supercritical side. Consequently, we may write:

$$h_{wave} = h_{film} \cdot \frac{\sqrt{1 + 8Fr_{film}^2} - 1}{2} \quad (4)$$

$$Fr_{film}^2 = \frac{(u_F - u_{film})^2}{g'h_{film}} \quad (5)$$

where h_{film} is the film height and h_{wave} is the wave height. So far, we have assumed channel flow, i.e. flow in a wide rectangular duct. For pipe flow, the expressions become slightly more complicated because of the pipe geometry, and an explicit analytical expression for h_{wave} cannot be obtained. However, it can be shown that simply replacing the liquid heights by $\alpha_l \cdot D$ yields a very good approximation. The equations then become:

$$\alpha_{l,wave} = \alpha_{l,film} \cdot \frac{\sqrt{1 + 8Fr_{film}^2} - 1}{2} \quad (6)$$

$$Fr_{film}^2 = \frac{(u_F - u_{film})^2}{g'D\alpha_{l,film}} \quad (7)$$

We may also note that by introducing the assumption of steady-state flow, the front velocity u_F can be assumed equal to the slug/wave tail velocity. We will henceforth refer to both these velocities to u_{wave} . From these equations, we see that for sufficiently high film Froude numbers, $\alpha_{l,wave}$ will exceed unity, meaning that the inertial forces are strong enough to sustain a wave that extends all the way to the top of the pipe, yielding a slug. However, if the film Froude number is small, $\alpha_{l,wave}$ can become smaller than unity, in which case the wave cannot reach the top of the pipe. In this case, we will only have a wave instead of a slug, and it is our thesis that this is the reason why we get wavy flow instead of slug flow for the lowest gas rates in Figure 3.

To include the effects discussed in the previous section, we amend the existing slug flow model (Unit Cell Model, or UCM) to model waves in addition to slugs. The pertinent feature of waves (compared to slugs) is that there is continuous gas at the top of the pipe. By generalizing the UCM equations to wavy flow, it can then be shown that the total average gas fraction in wavy flow equals:

$$\alpha_g = \frac{USG + \alpha_{dg,wave} (u_{wave} - u_{dg,wave}) + \alpha_{cg,wave} (u_{wave} - u_{cg,wave})}{u_{wave}} \quad (8)$$

Here, $\alpha_{dg,wave}$ is the fraction of dispersed bubbles in the wave, $u_{dg,wave}$ is the axial velocity of those bubbles, $\alpha_{cg,wave}$ is the fraction of continuous gas over the wave, $u_{cg,wave}$ is the associated velocity, and u_{wave} is the wave velocity. Figure 5 shows a schematic description of the pseudo slug model, indicating the meaning of the various parameters in equation (8).

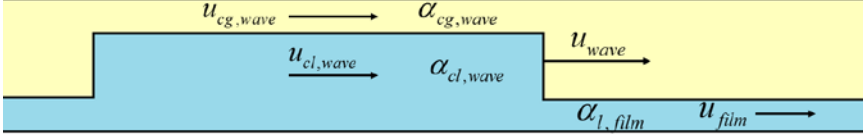


Figure 5: Schematic description of the pseudo slug model.

Lacking detailed measurements of all the quantities in equation (8), we need to make some assumptions in this model.

The main assumptions are:

1. The phase fraction and velocity of the gas bubbles in the wave $\alpha_{dg,wave}$ and $u_{dg,wave}$ can be calculated using the associated models for slug flow. These assumptions preserve continuity between slug flow and pseudo slug flow. The concentration of gas bubbles is typically small in pseudo slug flow (due to the small Froude number), hence these assumptions are not critical in terms of accuracy.
2. u_{wave} is equal to the slug bubble velocity for regular slug flow. This assumption preserves continuity between slug flow and pseudo slug flow, and is almost certainly valid near the slug flow transition. With the available measurements, it was however not possible to directly validate this assumption, because the distance between the gamma densitometers was too large to perform a cross-correlation and calculate the wave velocities (the waves are much shorter than typical slugs).
3. $u_{cg,wave}$ is equal to u_{wave} . This assumption, combined with the previous one, leads to total gas fractions that are equal to that in slug flow. This is based on the observation that the slug flow model predicts the holdup accurately in the pseudo slug flow domain, as seen in Figure 2 and Figure 3.
4. The fraction of continuous gas in the wave ($\alpha_{cg,wave}$) is equal to the $1 - \alpha_{l,wave}$ as given by equation (6) near the transition between slug flow and pseudo slug flow. This assumption is required for continuity between slug flow and pseudo slug flow. Far away from the transition, it was found that this assumption was inadequate, and that different treatment was required. This will be described below.

As mentioned in the previous paragraphs, the wave liquid fraction close to the transition to slug flow should be given by equation (6). It was however discovered that this expression did not work in all circumstances. The scenarios for which it tended to fail were:

- Froude numbers approaching unity, where the hydraulic jump model predicted small or zero wave heights. In such cases, it is believed that the waves may be roll waves, so that the wave fronts are not adequately described by the hydraulic jump equations. Consequently, a different approach is needed to calculate the wave height in these scenarios.
- Low pressure (low gas density), where slug flow was observed instead of pseudo slug flow, even for very low Froude numbers. This was primarily observed for atmospheric conditions, but we also found that the waves sometimes partially bridged the pipe cross section even at 20 bara pressure. At higher pressures, we did not see this.

A possible explanation for the latter observation may be that for "soft" low-pressure systems, local temporal variations in the flow can arise more easily than in a "stiff" high-pressure system. Specifically, at low pressure, the gas has a low density and thus low inertia, and a growing wave may then be able to decelerate the surrounding gas locally to form a slug. More generally, local flow variations can temporarily yield conditions that favour slug initiation, and once a slug is born, it may persist indefinitely because there will in these cases be sufficient liquid in front of it to survive (since the minimum slip criterion is fulfilled).

Based on these considerations, and general observations in the available experimental data, we arrived at the following expression for the wave height in pseudo slug flow:

$$h_{wave} = \max \left[\min \left(h_{jump}, D \right); h_{film} + R \left(\rho_g, \rho_l \right) \cdot \left(D - h_{film} \right) \right] \quad (9)$$

Here, h_{jump} refers to the liquid height corresponding to the liquid fraction given by equation (6). The function $R(\rho_g, \rho_l)$ is an empirical correlation that we withhold for confidentiality reasons. We may however impart that R approaches unity at low gas/liquid density ratios, so that slug flow prevails at low pressure. Although this is outside the scope of this paper, we can mention that atmospheric experiments at "pseudo slug conditions" ($h_{jump} < D$) show that the prevailing flow regime can indeed be slug flow, as opposed to pseudo slug flow. However, the associated slugs are "meta-stable", with large gas pockets entering the slugs, leading to frequent slug death and subsequent growth of surviving slugs. This is however a separate topic, and will not be addressed further in this paper.

4 PREDICTIONS WITH THE NEW MODEL

Figure 6 shows the same experimental data as Figure 3, but this time we have included simulation results obtained with the new model (implemented in LedaFlow 2.4), where the pseudo slug regime is included according to the equations supplied in the previous section. In these graphs we see that with the new model, both the flow regime predictions and the pressure drop predictions match the experiments well.

In Figure 7 we have included some more results, covering three pressures (20, 45 and 85 bara) and three liquid rates ($USL=1, 1.5$ and 2 m/s). The lines represent predictions with the new model, and we observe that the agreement with the measured pressure drop is much better than with LedaFlow 2.3 (Figure 2).

Finally, in Figure 8 we show the predicted holdup and pressure drop plotted against the measured values for LedaFlow 2.3 (left graphs) and LedaFlow 2.4 (right graphs). Here, we have also included data from the horizontal test section. The colour codes used in those plots are defined as follows:

For liquid holdup:

- Green = error < 0.05

For pressure drop:

- Green = error < 10% or error < 20 Pa/m
- Yellow = 10% < error < 20%
- Red = error > 20%

The holdup predictions are the same as before, which is ok, since they were already quite accurate for these conditions. The pressure drop predictions are however significantly better with the new model, as seen in the bottom graphs of Figure 8. Specifically, the number of "green" predictions increased from 41% to 92%, which is a big improvement.

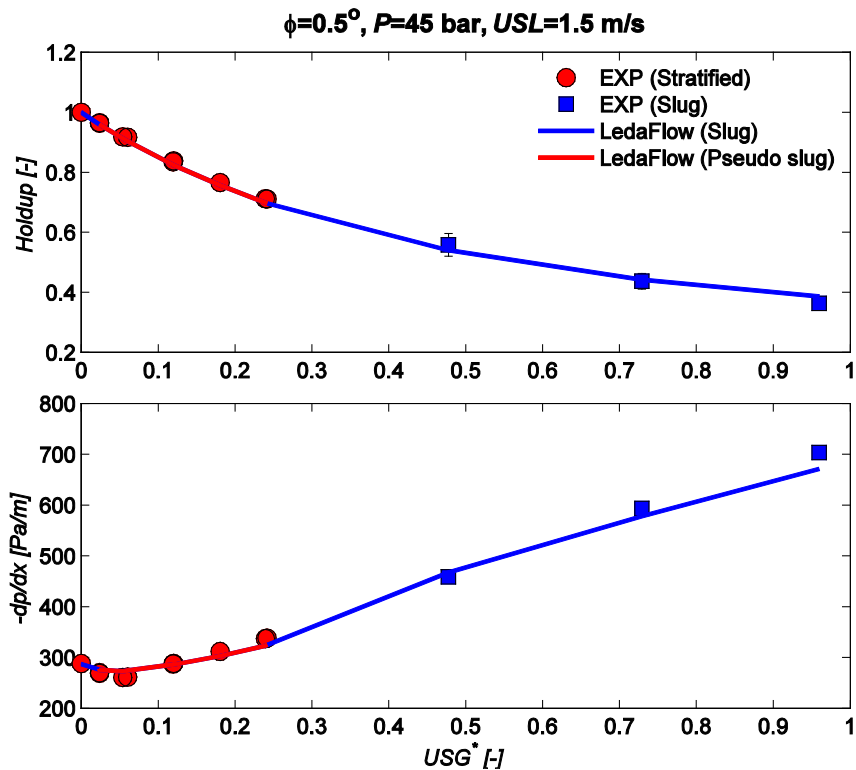


Figure 6: Holdup and pressure drop in the 0.5° section at 45 bara, with $USL=1.5$ m/s. The markers are the measured values, while the lines represent predictions with the new model (LedaFlow 2.4). The red colour means stratified (or pseudo slug) flow, while blue colour represents slug flow.

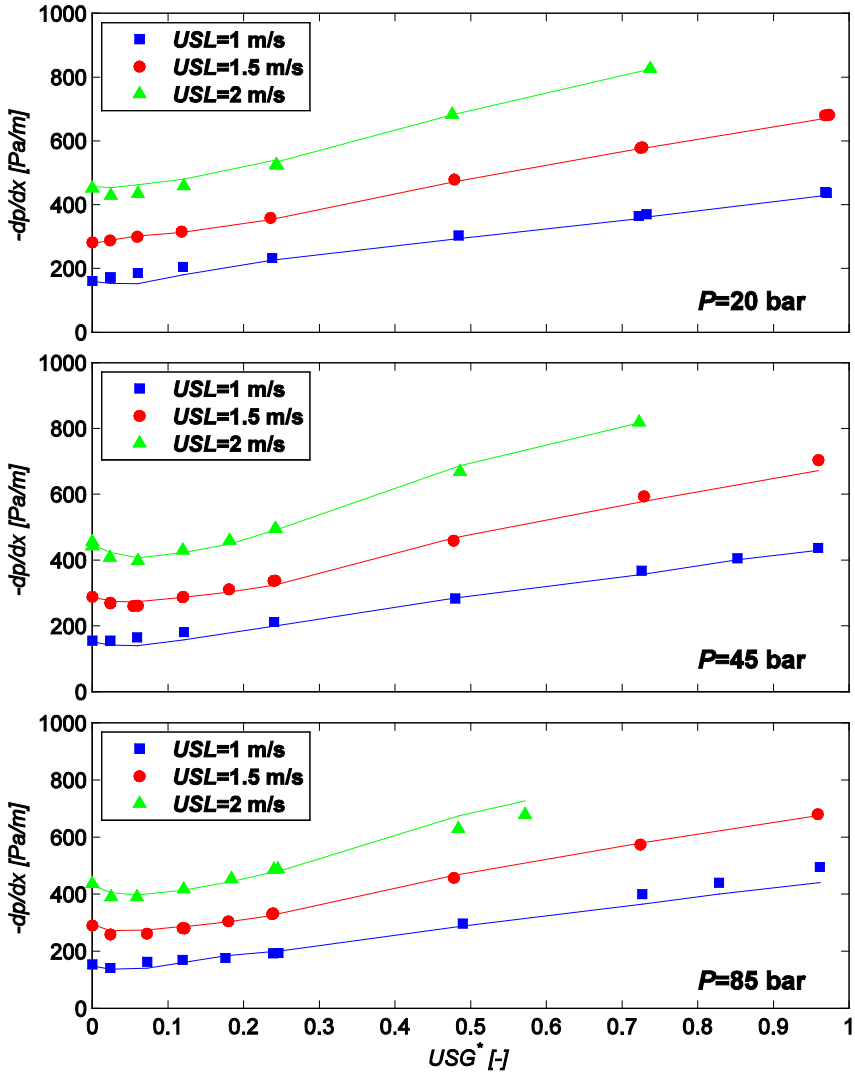


Figure 7: Pressure drop for USL=1, 1.5 and 2 m/s at pressures 20, 45 and 85 bara in the 0.5° pipe. The markers are the measured values, while the lines represent predictions with LedaFlow 2.4.

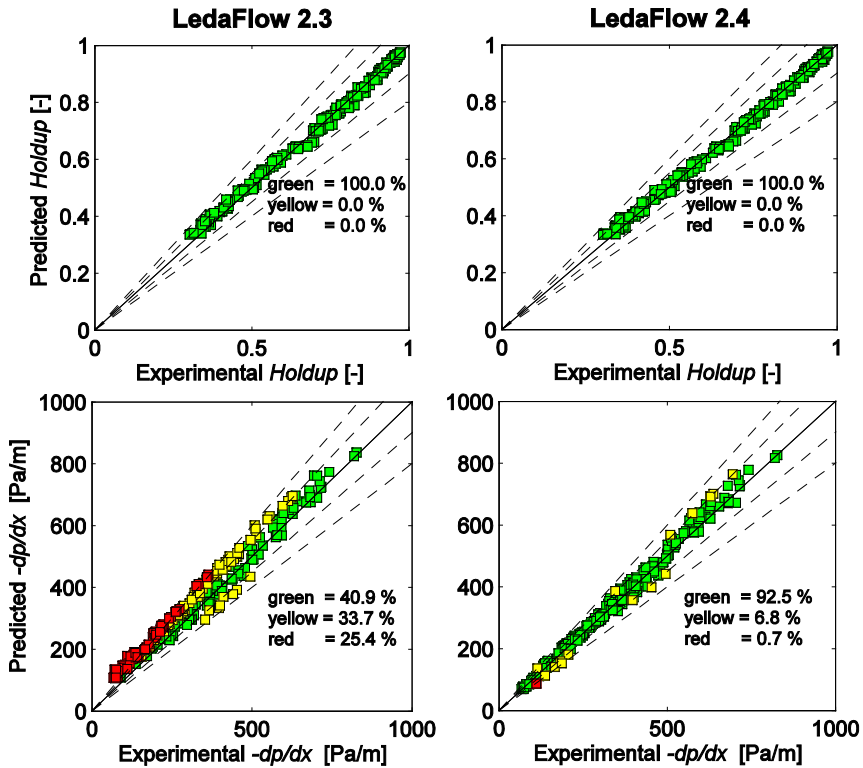


Figure 8: Predicted holdup and pressure drop plotted against the measured values for LedaFlow 2.3 (left graphs) and LedaFlow 2.4 (right graphs).

5 CONCLUSIONS

In this paper we have presented new two-phase flow data from experiments conducted at the SINTEF Multiphase Flow Laboratory at Tiller, Norway. The experiments were conducted at 20, 45 and 85 bara pressure, using Nitrogen as the gas phase, and Nexbase 3080 as the liquid phase. The liquid viscosity was in the range 86-99 cP, dependant on the system pressure.

The prevailing flow regime seen at low gas rates and high liquid rates was not slug flow, but a kind of pseudo slug flow, with large waves that were not able to fill the pipe cross-section entirely. Simulations with LedaFlow version 2.3 erroneously predicted these cases to be slug flow, which led to over-predictions in pressure drop.

Analysis of the experimental data revealed that under these conditions, slugs were not able to form because the waves did not have sufficient inertia to sustain a slug front. This limitation was not accounted for in the flow regime criteria in LedaFlow 2.3, so to improve the situation, the existing slug flow model in LedaFlow was amended to cover pseudo slug flow in addition to regular slug flow in LedaFlow 2.4. By introducing this new flow regime, the pressure drop predictions for viscous oil systems improved significantly.

6 ACKNOWLEDGEMENTS

The authors would like to thank Chevron, ENGIE, Shell, Statoil and TOTAL, who were the financial sponsors of the VOMS project [16] that supplied the experimental data shown in this paper. Furthermore, we would like to give special thanks to ENGIE and TOTAL, who financed the IMPROVED project [17], where the model concepts described in this paper were derived. Furthermore, we acknowledge the financial support from LedaFlow Technologies DA (co-owned by SINTEF, Kongsberg Digital, TOTAL and ConocoPhillips), who enabled us to implement the models developed in the IMPROVED project into LedaFlow. Finally, we would like to thank all the scientific and technical personnel at the SINTEF Multiphase Laboratory for all their dedicated work on the experiments.

7 REFERENCES

- [1] "LedaFlow," [Online]. Available: <http://www.ledaflow.com/>.
- [2] H. Alboudwarej et al, "Highlighting Heavy Oil," *Oilfield Review*, pp. 34-53, 2006.
- [3] J. Weisman, D. Duncan, J. Gibson and T. Crawford, "Effects of fluid properties and pipe diameter on two-phase flow patterns in horizontal lines," *Int. J. of Multiphase Flow*, vol. 5, no. 6, pp. 437-462, 1979.
- [4] T. Kago, T. Saruwatari, M. Kashima, S. Morooka and Y. Kato, "Heat transfer in horizontal plug and slug flow for gas-liquid and gas-slurry systems," *Journal of Chemical Engineering of Japan*, vol. 19, no. 2, pp. 125-131, 1986.
- [5] M. Nädler and D. Mewes, "Effects of the liquid viscosity on the phase distributions in horizontal gas-liquid slug flow," *International Journal of Multiphase Flow*, vol. 21, no. 2, pp. 253-266, 1995.
- [6] S. Nuland, "Bubble front velocity in horizontal slug flow with viscous Newtonian-, shear thinning- and Bingham fluids," in *Third International Conference on Multiphase Flow*. :, Lyon, France. , 1998.
- [7] B. Gokcal, An experimental and theoretical investigation of slug flow for high oil viscosity in horizontal pipes, PhD thesis, Tulsa: University of Tulsa, 2008.
- [8] J. Colmenares, P. Ortega, J. Padrino and J. L. Trallero, "Slug Flow Model for the Prediction of Pressure Drop for High Viscosity Oils in a Horizontal Pipeline," in *SPE Intl. Thermal Operations and Heavy Oil Symposium*, Porlamar, Venezuela, 2001.
- [9] K. Bendiksen, D. Malnes, R. Moe and S. Nuland, "The Dynamic Two-Fluid Model OLGA: Theory and Application," *SPE Production Engineering*, vol. 6, no. 2, 1991.
- [10] B. e. a. Jeyachandra, "Drift-Velocity Closure Relationships for Slug Two-Phase High-Viscosity Oil Flow in Pipes," *SPE Journal*, vol. 17, no. 2, pp. 593-601, 2012.
- [11] C. e. a. Kora, "Effects of High Oil Viscosity on Slug Liquid Holdup in Horizontal Pipes," in *Canadian Unconventional Resources Conference, Society of Petroleum Engineers*, Alberta, Canada, 2011.
- [12] B. Gokcal, A. Al-Sarkhi, C. Sarica and E. Al-Safran, "Prediction of Slug Frequency for High Viscosity Oils in Horizontal Pipes," in *Society of Petroleum EngineersSource SPE Annual Technical Conference and Exhibition*, New Orleans, Louisiana, 2009.

- [13] J. Nossen and C. Lawrence, "Pressure Drop in Laminar Slug Flow with Heavy Oil," in *BHR Group*, Banff, 2012.
- [14] I. Smith., J. Nossen and T. Unander, "Improved Holdup and Pressure Drop Predictions for Multiphase Flow with Gas and High Viscosity Oil," in *BHR Group*, Cannes, 2013.
- [15] I. E. Smith, F. N. Krampa, M. Fossen, C. Brekken and T. E. Unander, "Investigation of horizontal two-phase gas-liquid pipe flow using high viscosity oil: Comparison with experiments using low viscosity oil and simulations," in *15th International Conference on Multiphase production Technology*, Cannes, France, 2011.
- [16] J. Kjølås, I. E. Smith, R. Belt, T. E. Unander and C. Brekken, "VOMS Large scale experiments (confidential report)," SINTEF, Trondheim, 2012.
- [17] B. Lund, J. Kjølås, E. Krogh, A. A. Shmueli, C. Brekken, I. E. Smith and S. T. Johansen, "IMPROVED Models for two-phase flow with viscous oil (confidential report)," SINTEF, Trondheim, 2015.
- [18] Emerson. [Online]. Available: <http://www.emerson.com/en-us/automation/micro-motion>.
- [19] "National Institute of Standards and Technology," [Online]. Available: <http://webbook.nist.gov/chemistry/fluid/>.
- [20] K. Bendiksen and M. Espedal, "Onset of slugging in horizontal gas-liquid pipe flow," *International Journal of Multiphase Flow*, vol. 18, no. 2, pp. 237-247, 1992.
- [21] H. Chanson, *The hydraulics of open channel flow: an introduction*, Butterworth-Heinemann 2004, 2004.